

Improving AIRS radiance spectra in high contrast scenes using MODIS

Thomas S. Pagano*, Hartmut H. Aumann, Evan M. Manning, Denis A. Elliott, Steven E. Broberg
Jet Propulsion Laboratory, California Institute of Technology,
4800 Oak Grove Dr., Pasadena, CA 91109

ABSTRACT

The Atmospheric Infrared Sounder (AIRS) on the EOS Aqua Spacecraft was launched on May 4, 2002. AIRS acquires hyperspectral infrared radiances in 2378 channels ranging in wavelength from 3.7-15.4 μm with spectral resolution of better than 1200, and spatial resolution of 13.5 km with global daily coverage. The AIRS is designed to measure temperature and water vapor profiles for improvement in weather forecast accuracy and improved understanding of climate processes. As with most instruments, the AIRS Point Spread Functions (PSFs) are not the same for all detectors. When viewing a non-uniform scene, this causes a significant radiometric error in some channels that is scene dependent and cannot be removed without knowledge of the underlying scene. The magnitude of the error depends on the combination of non-uniformity of the AIRS spatial response for a given channel and the non-uniformity of the scene, but is typically only noticeable in about 1% of the scenes and about 10% of the channels. The current solution is to avoid those channels when performing geophysical retrievals. In this effort we use data from the Moderate Resolution Imaging Spectroradiometer (MODIS) instrument to provide information on the scene uniformity that is used to correct the AIRS data. For the vast majority of channels and footprints the technique works extremely well when compared to a Principal Component (PC) reconstruction of the AIRS channels. In some cases where the scene has high inhomogeneity in an irregular pattern, and in some channels, the method can actually degrade the spectrum. Most of the degraded channels appear to be slightly affected by random noise introduced in the process, but those with larger degradation may be affected by alignment errors in the AIRS relative to MODIS or uncertainties in the PSF. Despite these errors, the methodology shows the ability to correct AIRS radiances in non-uniform scenes under some of the worst case conditions and improves the ability to match AIRS and MODIS radiances in non-uniform scenes.

Keywords: AIRS, Spatial, Co-Registration, Clouds

1. INTRODUCTION

1.1. AIRS and MODIS on Aqua

The Atmospheric Infrared Sounder (AIRS) measures atmospheric temperature and water vapor profiles from space. AIRS resides on the EOS Aqua spacecraft launched in May 2002. The AIRS is a “facility” instrument developed by NASA as an experimental demonstration of advanced technology for remote sensing and the benefits of high resolution infrared spectra to weather forecasting and atmospheric process studies. The AIRS, in conjunction with the Advanced Microwave Sounding Unit (AMSU), produces temperature profiles with 1K/km accuracy on a global scale, as well as water vapor profiles and trace gas amounts for CO_2 , CO, SO_2 , O_3 and CH_4 ¹. AIRS continues to provide high forecast impact^{2,3} and is widely used for scientific investigations⁴ including climate model validation^{5,6}.

Figure 1 shows a schematic of the AIRS scan pattern and flight geometry. AIRS scans a single nearly circular 13.5 km Instantaneous Field of View (IFOV) in the cross-track direction as it traverses the orbit. A total of 90 IFOV's are obtained per scan. After 3 scans, a set of 3x3 AIRS

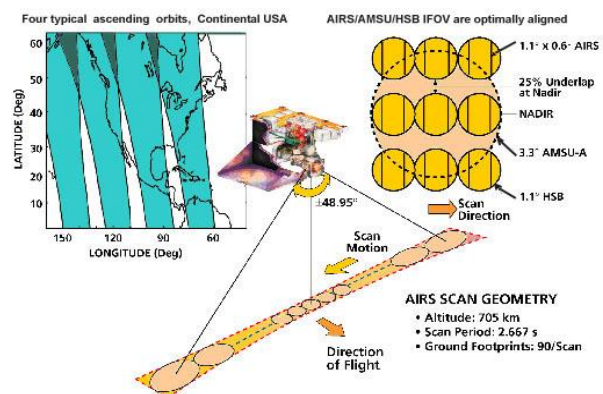


Figure 1. AIRS scans cross-track with 90 IFOV's. The IFOV's rotate with scan producing a complicated PSF.

*thomas.s.pagano@jpl.nasa.gov, phone: (818) 205-4702,
<http://airs.jpl.nasa.gov>

observations are matched to a single 45 km Advanced Microwave Sounding Unit (AMSU) footprint prior to being used together in a geophysical retrieval of temperature and water vapor. Each of the 90 IFOV's for AIRS contains a complete spectrum of the 2378 infrared channels ranging from 3.7 μm to 15.4 μm . AIRS has a view to space, an on-board blackbody and parylene spectral calibrator (used pre-flight). In-flight spectral calibration is performed using the upwelling earth scene.

The AIRS radiometric calibration is excellent with an accuracy of better than 200 mK for most channels⁷. AIRS spectral calibration is extremely stable, with less than 10 ppm drift over the life of the mission (<0.5% of the channel spectral resolution). AIRS in-flight radiometric and spectral calibration were updated recently showing an increase in stability with time⁸. We have seen no evidence of a change in spatial resolution or boresight pointing knowledge (< 1km at nadir) in AIRS imagery from what was determined shortly after launch^{9,10}.

The MODIS instrument operates on the same spacecraft as the AIRS, the NASA Aqua polar orbiting satellite, and scans cross-track like AIRS, but with nominally 10 detectors aligned along-track for each 1km band, and correspondingly more for bands with 500m and 250 m spatial resolution¹¹. MODIS has 36 spectral bands ranging in wavelength from 0.4 μm – 14.4 μm . Only one band is used in this analysis, Band 31 centered at 1.1 μm , and represents a “window” channel with low water vapor absorption. MODIS radiometric accuracy is better than 1% in the LWIR, or about 1K¹². MODIS geolocation accuracy is better than 55 m¹³.

1.2. Spatial Inhomogeneity Impact to Operations and Science

AIRS is an infrared grating spectrometer and is radiometrically calibrated in-orbit under spatially uniform conditions using a full aperture On-Board Blackbody Calibrator (OBC) and a full aperture space view. When the spatial response of the instrument varies amongst the spectral channels or bands (also known as misregistration), radiometric differences result when viewing spatially inhomogeneous scenes. These differences represent a radiometric error if uncorrected.

To date, the way AIRS level 1B radiances are used, there has not been an issue with radiometric errors due to scene inhomogeneity and misregistration. National Weather Prediction (NWP) centers typically filter cloudy radiance data during AIRS radiance assimilation since cloud hyperspectral infrared radiative properties are not yet well represented in the operational forecast models. They also use a subset of AIRS channels that are the least impacted by spatial response nonuniformity. AIRS L1B users should consult the AIRS Level 1B QA Quick Start guide (http://disc.sci.gsfc.nasa.gov/AIRS/documentation/v6_docs) to avoid use of channels with high noise or high centroid values or bad spectral response. Typically, investigations requiring intercomparison of AIRS and MODIS radiance data are more affected by spectral response function errors than scene inhomogeneity effects¹⁴. The AIRS project has developed a Level 1C (L1C) product that replaces dead or bad pixels with a PC reconstruction and flags them so users are aware of the substitution¹⁵. Level 2 retrieval algorithms use cloud clearing at the 3x3 level, again with the most uniform channels and have shown no impact from this effect. Typically the impact is on the order of a few km (1/10th of an AIRS field of view), when Level 2 data products are 45 km at nadir. Level 3 products are significantly coarser at 1°x1° (approximately 110 km at nadir).

More recently, as we attempt to improve the spatial resolution of the AIRS Level 2 products, and use data closer to cloudy boundaries, we find that understanding the errors due to spatial inhomogeneity and removing them to the extent possible is important to progress. Single pixel retrievals are available with new ones under development that will be more impacted by scene inhomogeneity effects since the result will not have the benefit of spatial averaging. Cloud clearing and retrievals in cloudy regions for single footprint retrievals are highly sensitive to scene inhomogeneity and misregistration. Reducing scene dependent radiometric errors in the Level 1B up front, rather than in the retrievals is preferred, but error characterization is essential.

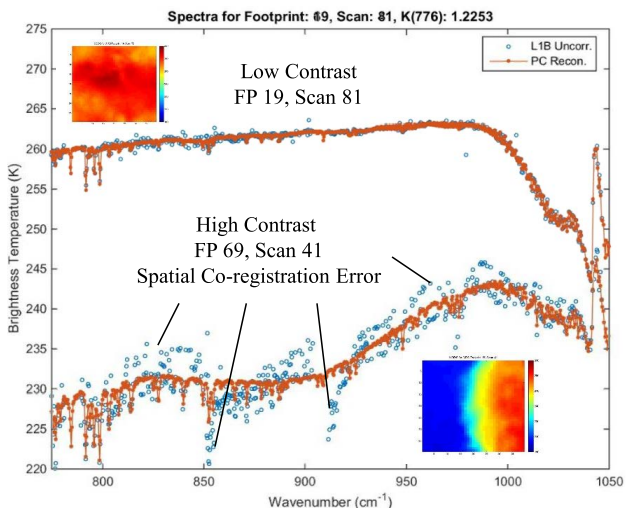


Figure 2. AIRS Spectra for low contrast (upper), and high contrast (lower) scenes. Insert image is from MODIS over AIRS PSF region. Variation in PSF introduces channel dependent error in spectra in high contrast scenes.

To highlight the issue with misregistration, Figure 2 shows two sample spectra from AIRS acquired on April 1, 2014. The radiance spectra have been converted to brightness temperature in the figure. We show the 800-1050 cm^{-1} spectral range where the effect is most prominent. The upper plot in Figure 3 shows a low-contrast, warm scene. In this plot, the channel-to-channel variability is small and compares well with a principal component (PC) reconstruction also shown in the figure for that spectrum. The PC reconstruction is trained on simulated spectra and applied to the radiance spectra shown prior to converting to brightness temperature. The channel-to-channel variability is low since the scene contrast is low, mitigating any issue with channel-to-channel PSF variability. The lower plot in Figure 3 shows a high contrast scene. Here we see significant differences compared to the PC reconstruction. Differences can be as high as 15 degrees.

In prior work we showed how the AIRS PSF's can improve the intercomparison of radiances between AIRS and MODIS in non-uniform scenes^{16,17}. In this work we use the AIRS spatial response and the MODIS radiance data to actually correct radiometric errors in the AIRS data due to scene inhomogeneity and misregistration in affected channels and footprints. We use knowledge of the AIRS in-flight spatial response, or Point Spread Function (PSF), MODIS radiances, and AIRS and MODIS geolocation data to correct AIRS radiances in non-uniform scenes.

2. METHODOLOGY

2.1. Radiometric Normalization

Given knowledge of the spatial response of AIRS (PSF's) and the scene radiance distribution (from MODIS) we should be able to correct the negative effects of variable co-registration amongst all channels. We do this by multiplying the calibrated radiance by a factor that corrects for the scene inhomogeneity and the variability in the AIRS response functions. The spatially averaged radiance from AIRS depends on the scene and AIRS spatial response:

$$L_{AIRS,i} = \frac{\sum_x \sum_y L_i(x,y) R_i(x,y)}{\sum_x \sum_y R_i(x,y)} \quad (1)$$

where

$$\begin{aligned} L_{AIRS,i} &= \text{AIRS LIB radiance in the } i^{\text{th}} \text{ channel (W/m}^2\text{-sr-}\mu\text{m)} \\ L_i &= \text{Scene radiance in the } i^{\text{th}} \text{ channel (W/m}^2\text{-sr-}\mu\text{m)} \\ R_i &= \text{AIRS Point Spread Function (unitless)} \\ x,y &= \text{Longitude and Latitude of the AIRS PSF Grid (deg)} \end{aligned}$$

If we know the scene radiance, we can correct for an irregular spatial profile by normalizing it to the signal that would result using an "average" spatial profile (i.e. Flat-Field AIRS Response)

$$L'_{AIRS,i} = \frac{\sum_x \sum_y R_i(x,y) \sum_x \sum_y L_i(x,y) R_o(x,y)}{\sum_x \sum_y L_i(x,y) R_i(x,y) \sum_x \sum_y R_o(x,y)} L_{AIRS,i} \quad (2)$$

where

$$\begin{aligned} L'_{AIRS,i} &= \text{Spatially Corrected AIRS Radiance in the } i^{\text{th}} \text{ channel (W/m}^2\text{-sr-}\mu\text{m)} \\ L_i &= \text{Scene radiance in the } i^{\text{th}} \text{ channel (W/m}^2\text{-sr-}\mu\text{m)}. \\ R_o &= \text{Average AIRS Point Spread Function over all channels} \end{aligned}$$

For the scene radiance, L_i , we use a MODIS window band radiance, L_M at 11.017 μm . At first we used the MODIS band closest in wavelength to the AIRS channel being corrected, but found that choice of band only leads to a change in the applied correction of less than 10%. This is most likely due to the fact that the scene contrast is very similar in most channels since the contrast is due to clouds and clouds have a slowly varying spectral signature. Use of a single MODIS band for all channels makes the operational implementation of the algorithm simpler.

If we wish to compare MODIS radiances and AIRS radiances, the MODIS radiance must also be weighted by the average AIRS PSF.

$$L'_M = \frac{\sum_x \sum_y L_M(x,y) R_o(x,y)}{\sum_x \sum_y R_o(x,y)} \quad (3)$$

2.2. Spatial Alignment

Before the correction algorithm is applied the PSF spatial grid must be aligned with the scan and track directions of AIRS. The PSF grid also must be scaled to the local latitude and longitude grid and centered on the AIRS footprint.

Rotation: The AIRS PSF's are acquired on a 39 x 39 element grid with increment 0.04°. They are acquired in the scan and track directions. For each IFOV, there is a unique angle, $\theta_{j,k}$, measured counter clockwise between the AIRS scan plane and the local parallel that can be calculated from the AIRS geolocation for the two points immediately adjacent to the IFOV in the along scan direction.

$$\tan(\theta_{j,k}) = \frac{dlat}{dlon} \quad (4)$$

where

$$dlat_{j,k} = [(lat_{j+1,k} - lat_{j,k}) + (lat_{j,k} - lat_{j-1,k})]/2 \quad (5)$$

$$dlon_{j,k} = [(lon_{j+1,k} - lon_{j,k}) + (lon_{j,k} - lon_{j-1,k})]/2 \quad (6)$$

and j is the scan direction index and k is the track direction index.

Scaling and Centering: We then need to scale the PSF grid to the latitude and longitude grid. We know the AIRS grid is acquired on 1.089° increments in the scan direction and can compute the corresponding scale factor between scan angle and latitude and longitude.

$$S_{j,k} = \frac{dlon_{j,k}/\cos(\theta_{j,k})}{1.089^\circ} \quad (7)$$

$$T_{j,k} = \frac{dlat_{j,k}/\sin(\theta_{j,k})}{1.089^\circ} \quad (8)$$

The resulting latitude and longitude grid of the PSF can now be computed with the rotation angle and scale factors above.

$$lon_{PSF,j,k,l,m} = x_{l,m} \cdot S_{j,k} \cdot \cos(\theta_{j,k}) - y_{l,m} \cdot T_{j,k} \cdot \sin(\theta_{j,k}) + lon_{j,k} \quad (9)$$

$$lat_{PSF,j,k,l,m} = x_{l,m} \cdot S_{j,k} \cdot \sin(\theta_{j,k}) + y_{l,m} \cdot T_{j,k} \cdot \cos(\theta_{j,k}) + lat_{j,k} \quad (10)$$

Where $x_{l,m}$, and $y_{l,m}$ are the angular coordinates (39 x 39) of the PSF from pre-flight testing and range from $-19 \cdot 0.04^\circ = -0.76^\circ$ to $+0.76^\circ$ in 0.04° increments.

Figure 3 shows the result of rotating the AIRS PSF grid to match the scan and track directions of the AIRS and MODIS instruments. The PSF grid is centered on the central AIRS pixel in the image. The next step is to resample the MODIS data to the AIRS PSF grid. We then have all the information in the right format to perform the summations in equation (2).

3. DATA

This section provides additional detail on the AIRS PSFs and the AIRS and MODIS data used in the analysis. All data are available at the NASA GES/DISC, <https://disc.gsfc.nasa.gov>

3.1. AIRS PSFs

AIRS has a complex optical system driven by the infrared linear detector array technology of the time of development (1990's). AIRS uses 17 individual linear arrays of detectors (modules) to cover the spectrum and multiple afocal relay telescopes in a pupil-imaging configuration to coregister all detectors to a single IFOV on the ground. Figure 4 shows the centroids of the AIRS

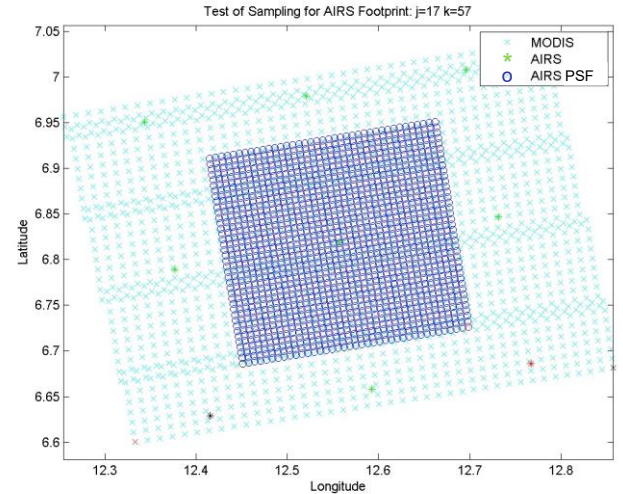


Figure 3. AIRS (*) and MODIS (x) data grid, and AIRS PSF grid projected on the ground (o). The black and red icons are the pixels of the first and last rows respectively in the first column of the AIRS and MODIS data files.

spatial response “tophat” functions acquired prior to launch with the instrument not scanning¹⁸. While accurate coregistration is achieved for the vast majority of channels, we see as much as 10% misregistration in some channels with the biggest deviation in the elevation (track) direction. Channels with detectors at the ends of modules show the largest deviations. The tophat functions for these channels are the most irregular, likely due to vignetting of the pupil.

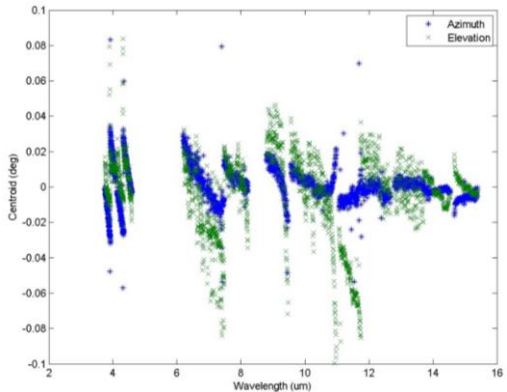


Figure 4. The centroids of the AIRS Tophat functions measured pre-flight can be off by as much as 0.1° (10% of a pixel) in elevation.

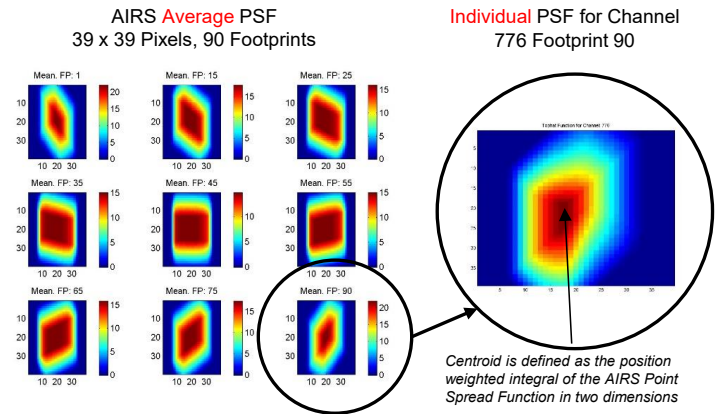


Figure 5. AIRS Point Spread Functions (PSF's), include static pre-flight “Tophat” measurements combined with the motion of the scan mirror.

The tophat functions are truncated, rotated and convolved with the integration blur to make an in-flight PSF for each channel and each footprint of the AIRS¹⁷. The average PSF over all AIRS channels is shown in Figure 5 for 9 representative footprints, as well as a PSF for channel 776 at the end of scan. We can see from the figure that the centroid for channel 776 (913.4 cm⁻¹, 10.59 μm) is considerably different than the average shown in the lower right corner of the 3 x 3 average footprints in the figure. The PSF's are oriented in the data file with scan and track as shown in Figure 6. We also show the orientations of the AIRS geolocation grid. In order to use the AIRS PSF's, they must first be rotated by 180° prior to use in equation 2 above.

3.2. AIRS and MODIS Data

To test the above correction algorithm, we look at data acquired from AIRS and MODIS on May 1, 2014 acquired over central Africa. We use the AIRS AIRIBRAD, and the MODIS MYD021KM fully calibrated radiance data products, and corresponding geolocation file for MODIS (geolocation is contained within the AIRS data file). AIRS granule 124 and MODIS granules 1220 and 1225 were used in the analysis. We use two MODIS granules to ensure we cover the entire region covered in the AIRS granule. The AIRS granule and one of two MODIS granules is shown in Figure 7.

The MODIS radiances are acquired over a significantly wider spectral bandpass than the AIRS data, however the normalization applied in equation 2 results in only the scene contrast as being significant, and mitigates the significant bias differences in the raw radiances. MODIS radiance data are converted from W/m²-sr-μm to mW/m²-sr-cm⁻¹ to be consistent with AIRS radiances.

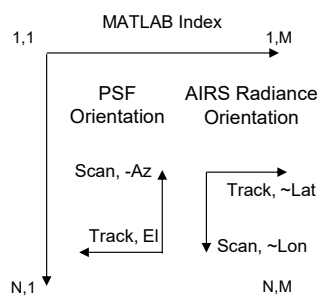


Figure 6. Orientation of PSF and AIRS radiance scan and track relative to MATLAB index.

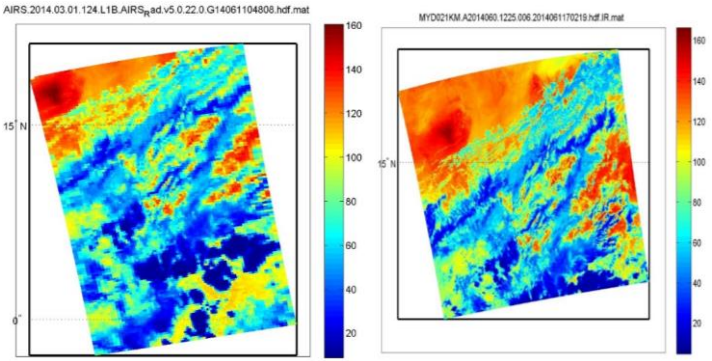


Figure 7. Granules used to demonstrate correction algorithm acquired May 1, 2014. (Left) AIRS Granule 124 channel 776 (Right) MODIS Granule 1225 Band 31 .

For each AIRS footprint, the closest MODIS footprint is found in the granule. Then a 40x40 grid of MODIS pixels around the AIRS pixel is fed into an interpolation routine to determine the value of the radiance at the location of the AIRS PSF projected on to the ground. Since each MODIS pixel is 0.08° , we are certain to cover all locations in the PSF grid (39×39 at 0.04°). The experiment was repeated using descending granules 148 for AIRS and 1450 for MODIS.

4. RESULTS

The resampled MODIS data, the AIRS PSF's and the AIRS radiances were used in equation (2) above to determine a corrected radiance for AIRS. The footprints with the greatest contrast were first used to see how well the result works on an individual footprint. Statistics were calculated for the worst spectral channels over all footprints, and for all footprints and all channels.

4.1. Single Footprint Results

Figure 8 shows radiances for the highest contrast footprint in the ascending granule for a region of the spectrum with the most atypical PSF's. Inset in Figure 8 is an image of the MODIS data within the AIRS PSF region. This figure is the same as Figure 2 but we have added the radiances for Level 1C (L1C) and for the MODIS corrected (MODIS Corr) AIRS L1B per equation (2) and a PC reconstruction. The AIRS L1C replaces dead or bad channels that exceed a threshold with a PC reconstruction. First we see that the significant outliers near 850 cm^{-1} and 910 cm^{-1} are eliminated in the MODIS corrected AIRS data. The L1C and the PC reconstructed data follow a similar curve but differ from the MODIS corrected AIRS radiances, particularly near 875 cm^{-1} and 1100 cm^{-1} . It is believed that the reconstruction produces a small bias in these regions as it attempts to fit the uncorrected AIRS data. Figure 9 shows the algorithm applied to a descending granule for AIRS and MODIS. Again, the reconstruction in L1C follows the uncorrected data resulting in small biases in the 900 cm^{-1} region.

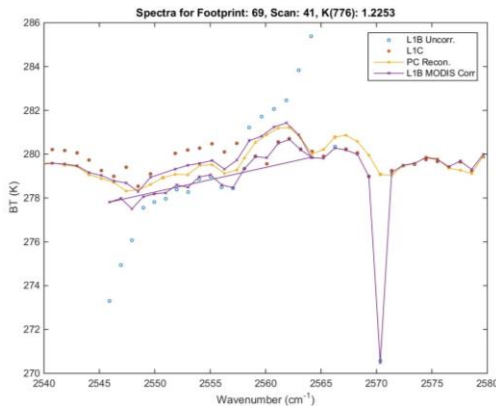


Figure 10. Same as Figure 7 for $2540\text{--}2480 \text{ cm}^{-1}$. Results demonstrate the effectiveness of the MODIS correction to the AIRS radiances.

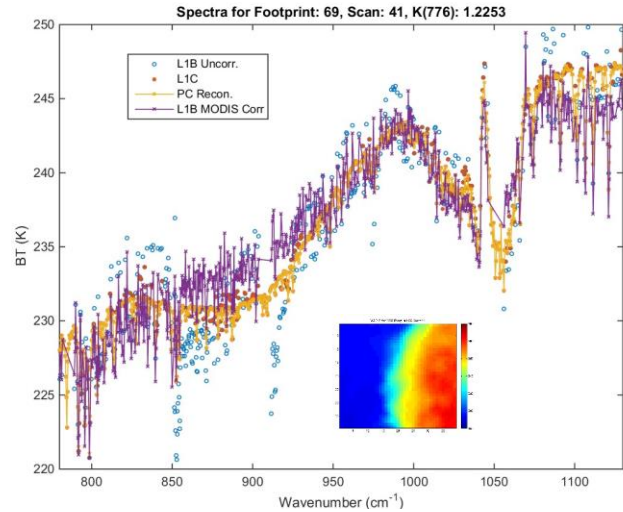


Figure 8. MODIS corrected AIRS spectrum, shows improvement for worst footprint in ascending granule compared to uncorrected, AIRS Level 1C and PC Reconstruction.

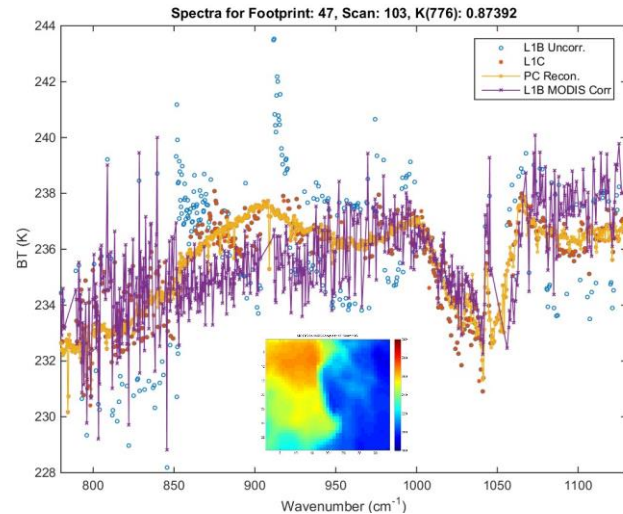


Figure 9. Same as Figure 8 for descending granule.

Figure 10 shows the algorithm applied to the 2560 cm^{-1} region. In this region, two AIRS detector modules cover the same region, or “overlap”. Level 1C does a good job of correcting the overlap but may introduce biases since the result appears to be higher than the reconstruction and the MODIS corrected radiances. The MODIS correction does not handle bad or dead detectors. As a solution to both problems, it may be possible to run the MODIS correction prior to running the radiances through L1C.

Not all AIRS footprints showed an improvement with the correction. Figure 11 shows the AIRS spectra for scan 3 footprint 41. This scene has high contrast but also a complex distribution. The fact that the correction does not work as well here indicates that we may have alignment problems between AIRS and MODIS that make more of a difference for this type of scene, or that we may have errors in our PSF. In the next iteration of this analysis, we will derive PSF's from AIRS and MODIS scene data thereby correcting for alignment errors between AIRS and MODIS and uncertainties in the PSF.

To further explore the question of how many channels improved, an experiment was performed where the LIC for AIRS ascending granule 124, May 1, 2014 (same as above) was processed on MODIS corrected AIRS radiances. The results showed that the overall number of cases requiring replacement was reduced by 12%, and of those that were due to scene inhomogeneity, a 90% reduction was observed. On the other hand, 11 channels actually had more footprints that required replacement with the LIC. For the footprint identified in Figure 11, LIC identified 3 channels that required replacement in the LIB, and 149 in the MODIS corrected AIRS radiances. We can look at the statistics of the entire granule to see how many channels improve or get worse and by how much.

4.2. Granule Level Statistics

The MODIS correction to the AIRS radiances was applied to all channels and footprints in the ascending granule (granule 140 for AIRS). This allows us to evaluate the improvement under normal scenes as well as highly spatially inhomogeneous scenes. It also allows us to look at the impact on other channels rather than the worst case channels.

Figure 12 shows the results for the worst case channel 776 considering all footprints in the granule. Here we plot the standard deviation of the difference between AIRS and MODIS as an indicator of radiometric error due to scene inhomogeneity. The standard deviation of AIRS-MODIS is plotted against the variability in the scene (as indicated by the MODIS standard deviation in the AIRS footprint). The standard deviation of AIRS-MODIS is calculated several ways as follows:

- 1) Uncorrected: AIRS L1B compared to MODIS L1B averaged over an ideal 1.1° circular AIRS PSF.
- 2) MODIS Corr: AIRS L1B compared to MODIS L1B weighted by the average AIRS PSF prior to averaging.
- 3) MODIS and AIRS Corr: AIRS L1B corrected using MODIS data and the AIRS PSF, compared to MODIS L1B weighted by the average AIRS PSF.
- 4) AIRS Level 1C compared to MODIS L1B weighted by the average AIRS PSF.
- 5) AIRS PC reconstruction compared to MODIS L1B weighted by the average AIRS PSF.

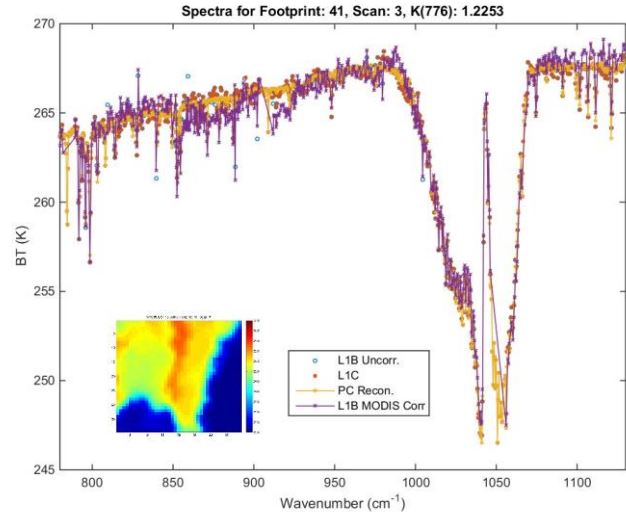
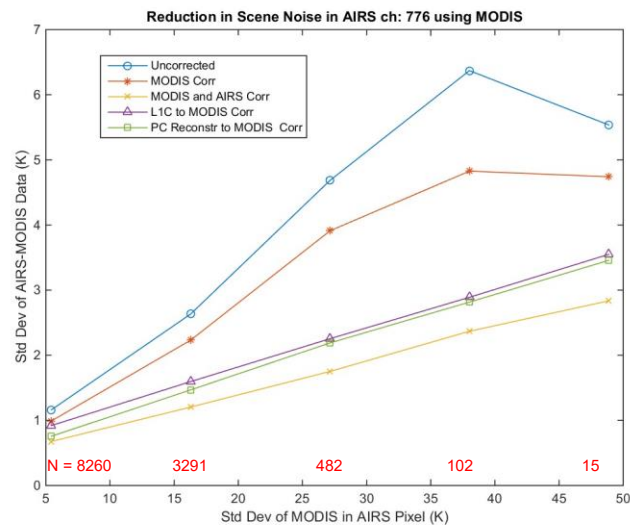


Figure 11. AIRS spectrum, uncorrected and corrected, for a footprint with high irregular inhomogeneity, compared to AIRS Level 1C and PC Reconstruction. In this footprint, the MODIS correction may have degraded the spectrum most likely due to alignment errors between the two instruments

We can look at the statistics of the entire granule to see how



between AIRS and MODIS brightness temperature vs standard deviation of MODIS data within the AIRS footprint for channel 776 (worst case channel).

The results show that for this channel, the benefit of weighting the MODIS data by the average AIRS PSF accounts for about 15-20% of the improvement in the comparison. We then see a big improvement when we correct the AIRS radiances using MODIS and the AIRS PSF for that channel. The improvement holds from low scene variability to the most highly variable scenes. The MODIS corrected AIRS radiances result in a slightly better match to the MODIS data than the LIC or the PC reconstruction.

Figure 13 shows the standard deviation of the difference between AIRS and MODIS as a function of footprint in the AIRS scan. The PSF has a high degree of variability as the scan progresses. This figure shows that the residual difference are radiometrically consistent with the PC reconstruction, indicating that our residual spatial inhomogeneity errors are small, since the reconstruction should be independent of these errors. The residual shape of the scan angle dependence between MODIS and AIRS could be due to a number of other effects, including AIRS radiometric bias vs scan angle (due to polarization effects), or MODIS Response vs Scan angle effects, also largely due to mirror polarization in the infrared¹².

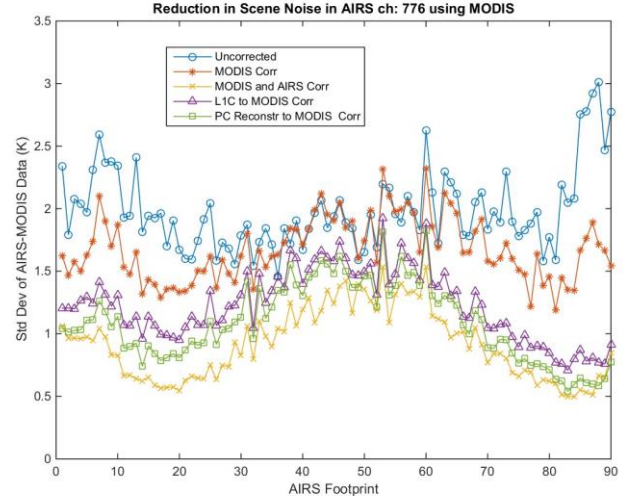


Figure 13. Standard deviation of the difference between AIRS and MODIS brightness temperature for ch. 776 vs AIRS footprint. No footprint dependence of the correction methodology is seen.

Figure 14 (left) shows the bias and standard deviation of the correction applied to all channels in the granule. The residual bias is less than 60 mK for all channels despite corrections of up to 10K in some channels. The nature of the residual biases has not been explored but in general the corrected data looks a little colder for channels with large corrections. Residual biases could be due to the use of only one granule in the analysis and may be different for different granules. Figure 14 (right) shows the standard deviation of the correction applied to the AIRS data. This figure gives an idea of how

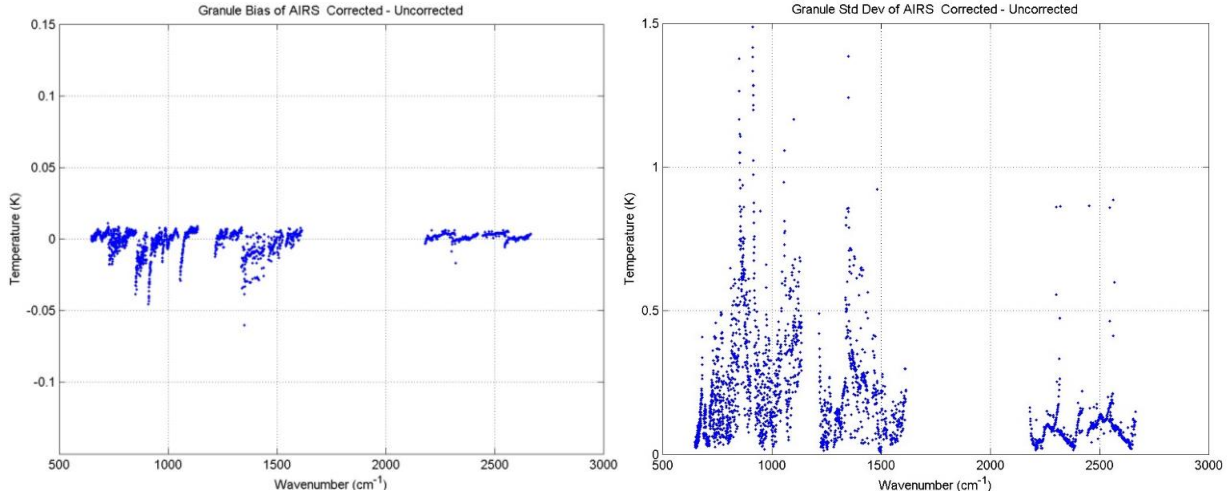


Figure 14. (Left). Residual bias between AIRS Corrected and Uncorrected brightness temperatures in granule 140. (Right) Standard deviation of the difference between AIRS Corrected and Uncorrected brightness temperatures in granule 140. Despite large corrections being applied (up to 10K), residual biases are low.

much correction is applied across the spectrum.

As a measure of the improvement or degradation, Figure 15 shows the difference in the standard deviation of the difference between AIRS uncorrected and MODIS and the standard deviation of the difference between AIRS corrected and MODIS.

$$\Delta T = \sigma[BT(L_{AIRS}) - BT(L'_{MODIS})] - \sigma[BT(L'_{AIRS}) - BT(L'_{MODIS})]$$

This difference, if positive, represents the improvement in the variability between AIRS and MODIS. Even though the variability depends on the contrast difference between the individual AIRS band and the MODIS band, an improvement is consistent with less scene variability due to scene inhomogeneity. All channels have ΔT between -0.15K and 1.2K, with apparent noise on the order of < 50 mK. Less than 10 channels have statistically significant increase in variability and may be due to uncertainties in the PSF or alignment differences. No correction for alignment difference between AIRS and MODIS was made in this analysis.

PSF uncertainties can come from the fact that the pre-flight test data were acquired in a particular state where A and B detectors were “on” for those channels where both detectors were “good”. Some channels have degraded and are now in an A only or B only state with unverified PSFs. Alignment and PSF uncertainties will be improved in the next version through training the PSF on the MODIS radiances.

5. SUMMARY AND CONCLUSIONS

A method has been developed to reduce the effect of scene inhomogeneity and instrument misregistration on the calibrated radiance spectra in the AIRS instrument. The problem manifests as discontinuities in the spectrum with scenes that have high contrast. Affected channels are those with the most asymmetry in their PSFs. The process involves first aligning the AIRS PSF's to the AIRS scan and track directions, and resampling the MODIS to the AIRS PSF's. The AIRS radiances are then corrected by multiplying by the theoretical response with an average PSF, and dividing out the theoretical response for the individual PSF of the channel being corrected. The worst affected channels in AIRS are improved considerably with a noise reduction of greater than 5x in the most inhomogeneous scenes. The method works well in most channels showing a reduction in variability relative to MODIS at the granule level, however, a few channels showed an increase. Most channels with degradation show an increase in variability of less than 150 mK and may be due to the introduction of random noise by the process, but may also be due to uncertainties in the PSF or alignment with MODIS in these channels. In flight the A/B redundancy configuration (AB-state) has changed several times throughout the mission and it is possible the PSF's are no longer representative for some channels. Additionally, small misalignments between AIRS and MODIS have not been corrected in this analysis. Despite the few channels that are slightly degraded, the vast majority of channels are improved with this method. With further refinements, we hope this work will facilitate use of the AIRS data in non-uniform scenes, and the use of MODIS data with AIRS data for scientific investigations in all scene types.

6. ACKNOWLEDGEMENTS

The research was carried out at the Jet Propulsion Laboratory, California Institute of Technology, under a contract with the National Aeronautics and Space Administration (NASA).

REFERENCES

- [1] Susskind, J., J. M. Blaisdell, and L. Iredell, “Improved methodology for surface and atmospheric soundings, error estimates, and quality control procedures: the AIRS science team version-6 retrieval algorithm,” *J. Appl. Remote Sens.* 8(1), 084994 (2014).
- [2] Jing, Zheng, L. I. Jun, Timothy J. Schmit, L. I. Jinlong, and L. I. U. Zhiquan. "The Impact of AIRS Atmospheric Temperature and Moisture Profiles on Hurricane Forecasts: Ike (2008) and Irene (2011)." *Advances in Atmospheric Sciences*, 32(3), 319-335 (2014).
- [3] Boullot, N., Rabier, F., Langland, R., Gelaro, R., Cardinali, C., Guidard, V., Bauer, P. and Doerenbecher, A., “Observation impact over the southern polar area during the Concordiasi field campaign.”, *Q.J.R. Meteorol. Soc.* (2014)

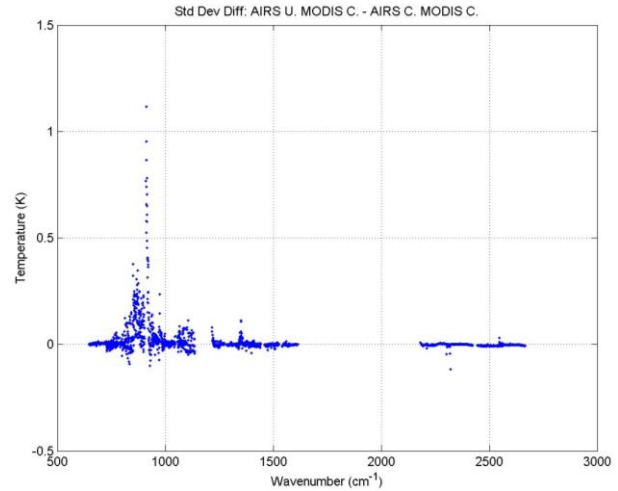


Figure 15: Difference in standard deviations between AIRS and MODIS, corrected and uncorrected. Not all channels improve with the correction (positive difference), and may be due to uncertainties in the PSF or alignment between MODIS and AIRS.

- [4] Pagano, T. S., M.T. Chahine, E.J. Fetzer, "The Atmospheric Infrared Sounder (AIRS) on the NASA Aqua Spacecraft: a general remote sensing tool for understanding atmospheric structure, dynamics and composition", Proc. SPIE 7827 (2010).
- [5] Pierce D. W., T. P. Barnett, E. J. Fetzer, P. J. Gleckler, "Three-dimensional tropospheric water vapor in coupled climate models compared with observations from the AIRS satellite system", Geophys. Res. Lett., 33, L21701 (2006)
- [6] Dessler, A. E., Z. Zhang, and P. Yang, "Water-vapor climate feedback inferred from climate fluctuations, 2003-2008", Geophys. Res. Lett., 35, L20704 (2008).
- [7] Pagano, T. S., H. Aumann, D. Hagan, K. Overoye, "Pre-Launch and In-flight Radiometric Calibration of the Atmospheric Infrared Sounder (AIRS)," IEEE TGRS, 00136-2002 (2002)
- [8] Pagano, T.S., Broberg, S., Aumann, H., Elliott, D., Manning, E., Strow, L, "Performance Status of the Atmospheric Infrared Sounder Ten Years after Launch", Proc. SPIE 8507 (2012)
- [9] Gregorich, David T., and Hartmut H. Aumann. "Verification of AIRS boresight accuracy using coastline detection." Geoscience and Remote Sensing, IEEE Transactions, 41(2), 298-302 (2003).
- [10] Pagano, T., H. Aumann, S. Gaiser, D. Gregorich, "Early Calibration Results from the Atmospheric Infrared Sounder (AIRS) on Aqua", Proc. SPIE 4891 (2002).
- [11] Barnes, W., T. Pagano, V. Solomonson, "Prelaunch Characteristics of the Moderate Resolution Imaging Spectroradiometer (MODIS) on EOS-AM1", IEEE Transactions on Geoscience and Remote Sensing, 36(4) (1998)
- [12] Xiong, X., et al., "Results and Lessons from MODIS Thermal Emissive Bands Calibration: Pre-launch to On-orbit", Proc. SPIE 6296 (2006)
- [13] Wolfe, R., M. Nishihama, "Trends in MODIS geolocation error analysis", Proc. SPIE 7452 (2009)
- [14] Schreier, M. M., B. H. Kahn, A. Eldering, D. A. Elliott, E. Fishbein, F. W. Irion, and T. S. Pagano. "Radiance comparisons of MODIS and AIRS using spatial response information." Journal of Atmospheric and Oceanic Technology 27(8), 1331-1342 (2010).
- [15] Manning, E., H. Aumann, A. Behrangi, "AIRS Level-1C and applications to cross-calibration with MODIS and CrIS", Proc. SPIE 9218 (2014)
- [16] Pagano, T. S. et. al., "Improving AIRS Spatial Co-registration by Resampling", Proc. SPIE 5890 (2005)
- [17] Elliott, D., T. Pagano, H. Aumann, "The Impact of the AIRS Spatial Response on Channel-To-Channel and Multi-Instrument Data Analyses", Proc. SPIE 6296 (2006)
- [18] Pagano, T. S., H. Aumann, L. Strow, "Pre-Launch Performance Characteristics of the Atmospheric Infrared Sounder", Proc. SPIE 4169 (2000)

-
- [1] ¹ Susskind, J., J. M. Blaisdell, and L. Iredell, "Improved methodology for surface and atmospheric soundings, error estimates, and quality control procedures: the AIRS science team version-6 retrieval algorithm," *J. Appl. Remote Sens.* 8(1), 084994 (2014).
- [2] ² Jing, Zheng, L. I. Jun, Timothy J. Schmit, L. I. Jinlong, and L. I. U. Zhiquan. "The Impact of AIRS Atmospheric Temperature and Moisture Profiles on Hurricane Forecasts: Ike (2008) and Irene (2011)." *Advances in Atmospheric Sciences*, 32(3), 319-335 (2014).
- [3] ³ Boullot, N., Rabier, F., Langland, R., Gelaro, R., Cardinali, C., Guidard, V., Bauer, P. and Doerenbecher, A., "Observation impact over the southern polar area during the Concordiasi field campaign.," *Q.J.R. Meteorol. Soc.* (2014).
- [4] ⁴ Pagano, T. S., M.T. Chahine, E.J. Fetzer, "The Atmospheric Infrared Sounder (AIRS) on the NASA Aqua Spacecraft: a general remote sensing tool for understanding atmospheric structure, dynamics and composition", *Proc. SPIE 7827* (2010).
- [5] ⁵ Pierce D. W., T. P. Barnett, E. J. Fetzer, P. J. Gleckler, "Three-dimensional tropospheric water vapor in coupled climate models compared with observations from the AIRS satellite system", *Geophys. Res. Lett.*, 33, L21701 (2006)
- [6] ⁶ Dessler, A. E., Z. Zhang, and P. Yang, "Water-vapor climate feedback inferred from climate fluctuations, 2003-2008", *Geophys. Res. Lett.*, 35, L20704 (2008).
- [7] ⁷ Pagano, T. S., H. Aumann, D. Hagan, K. Overoye, "Pre-Launch and In-flight Radiometric Calibration of the Atmospheric Infrared Sounder (AIRS)," *IEEE TGRS*, 00136-2002 (2002)
- [8] ⁸ Pagano, T.S., Broberg, S., Aumann, H., Elliott, D., Manning, E., Strow, L, "Performance Status of the Atmospheric Infrared Sounder Ten Years after Launch", *Proc. SPIE 8507* (2012)
- [9] ⁹ Gregorich, David T., and Hartmut H. Aumann. "Verification of AIRS boresight accuracy using coastline detection." *Geoscience and Remote Sensing, IEEE Transactions*, 41(2), 298-302 (2003).
- [10] ¹⁰ Pagano, T., H. Aumann, S. Gaiser, D. Gregorich, "Early Calibration Results from the Atmospheric Infrared Sounder (AIRS) on Aqua", *Proc. SPIE 4891* (2002).
- [11] ¹¹ Barnes, W., T. Pagano, V. Solomonson, "Prelaunch Characteristics of the Moderate Resolution Imaging Spectroradiometer (MODIS) on EOS-AM1", *IEEE Transactions on Geoscience and Remote Sensing*, 36(4) (1998)
- [12] ¹² Xiong, X., et al., "Results and Lessons from MODIS Thermal Emissive Bands Calibration: Pre-launch to On-orbit", *Proc. SPIE 6296* (2006)
- [13] ¹³ Wolfe, R., M. Nishihama, "Trends in MODIS geolocation error analysis", *Proc. SPIE 7452* (2009)
- [14] ¹⁴ Schreier, M. M., B. H. Kahn, A. Eldering, D. A. Elliott, E. Fishbein, F. W. Irion, and T. S. Pagano. "Radiance comparisons of MODIS and AIRS using spatial response information." *Journal of Atmospheric and Oceanic Technology* 27(8), 1331-1342 (2010).
- [15] ¹⁵ Manning, E., H. Aumann, A. Behrangi, "AIRS Level-1C and applications to cross-calibration with MODIS and CrIS", *Proc. SPIE 9218* (2014)
- [16] ¹⁶ Pagano, T. S. et. al., "Improving AIRS Spatial Co-registration by Resampling", *Proc. SPIE 5890* (2005)
- [17] ¹⁷ Elliott, D., T. Pagano, H. Aumann, "The Impact of the AIRS Spatial Response on Channel-To-Channel and Multi-Instrument Data Analyses", *Proc. SPIE 6296* (2006)
- [18] ¹⁸ Pagano, T. S., H. Aumann, L. Strow, "Pre-Launch Performance Characteristics of the Atmospheric Infrared Sounder", *Proc. SPIE 4169* (2000).